JOURNAL OF MATERIALS SCIENCE **38** (2003) 1507–1511

Growth, electrical and structural characterization of β-GaSe thin films

M. PARLAK
Department of Physics, Middle East Technical University, 06531 Ankara, Turkey

A. F. QASRAWI
Faculty of Engineering, Atilim University, 06836 Ankara, Turkey
E-mail: atef_qasrawi@atilim.edu.tr

Ç. ERÇELEBI
Department of Physics, Middle East Technical University, 06531 Ankara, Turkey

GaSe thin films were deposited onto the glass substrates kept at 200° and 300°C by the thermal evaporation of GaSe crystals under the pressure of 10^{-5} Torr. X-ray analysis of the films revealed that films grown at 200°C are amorphous in nature while the films grown at 300°C are polycrystalline β-GaSe. The temperature dependent electrical conductivity measurements in the region of 320–100 K for the films grown at 300°C showed that the transport mechanisms are the thermionic emission of charged carriers and the variable range hopping above and below 180 K, respectively. Space charge limited current (SCLC) studies have also been performed on these films through the current-voltage measurements at different temperatures and a dominant hole trap at 0.233 eV from the top of the valance band with a trap density of $\sim 1.6 \times 10^{11}$ cm^{-3} is identified. © *2003 Kluwer Academic Publishers*

1. Introduction

GaSe, layered semiconductor of III–VI group, has distinct structural, electrical and optical properties which are not found in more traditional group IV (Si, Ge), III–V (GaAs, AlAs, etc.) or II–VI (ZnSe, CdTe, etc.) materials. A layer of GaSe consists of two Ga and two Se sublayers in the sequence of Se—Ga—Ga—Se, where the Se—Ga and Ga—Ga bonds are covalent in the layers and the Se—Se bond between adjacent four atomic layers is due to van der Walls forces [1]. It is important that the cleaved surface has no dangling bonds and no surface states, in contrast with the surface of three dimensional materials. Therefore, GaSe single crystals were used for different device applications such as the base material of the heterojuntions with the window layers of SnO_2, ITO, In_2O_3 or as the window material together with the absorber layers such as InSe, CdTe, GaAs, Si etc. [2]. MIS and Schottky barrier photovoltaic devices [3, 4] and semiconductor detectors made with GaSe [5–7] were also studied.

Growth [8], crystal structure [9], electrical [10–14] and optical [15] properties of GaSe single crystals have been investigated in detail. Eventhough for many device applications, thin film materials are desirable, to our knowledge limited number of studies have been reported on the GaSe thin films. Structural properties of vacuum deposited GaSe thin films and the influence of the substrate temperature and deposition rate on the film structure were investigated [16]. The electrical and structural properties of GaSe thin films obtained by evaporation of Ga_2Se_3 and GaSe have been reported elsewhere [17]. Ga_2Se_3 and GaSe thin films grown on GaAs(100) and Si(111) substrates respectively by molecular beam epitaxy have been studied and found to be epitaxial [18, 19].

The properties of thin films strongly depend on the deposition conditions as well as the technique used. The detail investigation on the electrical and structural properties of the deposited films is essential for possible device applications. In this paper, the results of the structural and electrical characterization of the vacuum deposited GaSe thin films onto glass substrates at different temperatures are reported.

2. Experimental details

Powdered GaSe single crystals were used as the thermal evaporation source material. The stoichiometric composition of the source material was around 48.16% gallium and 51.84% selenium. The crystal powder was placed in quartz ampoule which was wound with molybdenum heating coil and heated up to 960°C under a pressure of 10^{-5} Torr. The films were evaporated onto ultrasonically cleaned glass substrates in Hall-bar and Van der Pauw shapes using appropriate masks for electrical measurements. The substrates were maintained at substrate temperatures of 200°C and 300°C for different evaporation cycles. The thickness of all the films was kept around 1 μm.

Electrical contacts were obtained by the evaporation of indium. The ohmic behavior of the contacts was

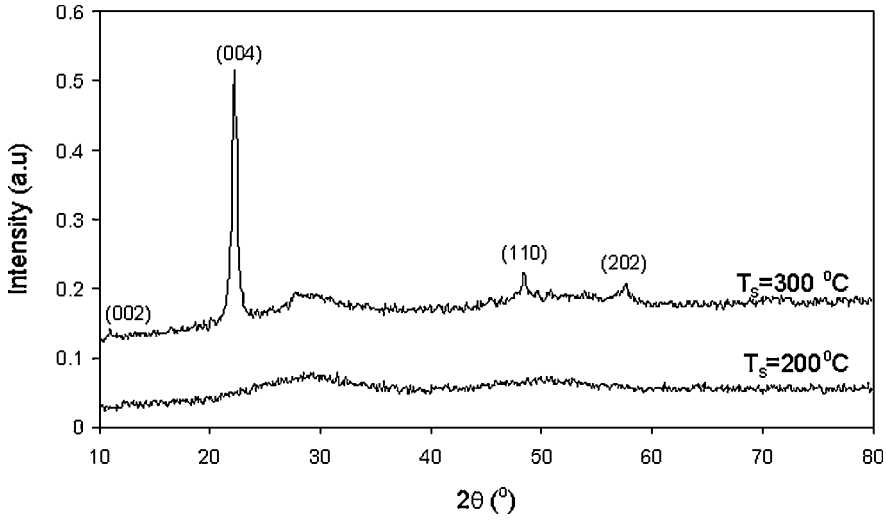

Figure 1 The X-ray diffraction patterns for GaSe thin films grown at $T_s = 200°C$ and $T_s = 300°C$.

confirmed by the linear variation of the current-voltage (I–V) characteristics up to 10 V which was independent of the reversal of the applied bias. The details of the temperature dependent resistivity and mobility measurements are described elsewhere [20, 21]. The I–V measurements at different temperatures for SCLC studies were done using the two evaporated In electrodes onto the film surface with a spacing of 0.15 cm and an area of $\sim$0.05 cm^2. The X-ray diffractograms were recorded using a Philips PW-1840 diffractometer equipped with Cu K_α radiation of average wavelength 1.54178 °A at a scan speed of 0.02° 2θ/s. The peak identification and the lattice parameters were obtained by using a TREOR 92 computer software.

3. Results and discussion

3.1. Structural analysis

In this work, the XRD technique is used to determine the structure, the phases present and the orientation of the deposited GaSe thin films. Typical X-ray diffraction patterns for the films grown at $T_s = 200°C$ and films grown at $T_s = 300°C$ are illustrated in Fig. 1. The patterns obtained from the films grown at $T_s = 200°C$ shows no peaks implying that these samples are amorphous in nature, whereas films grown at $T_s = 300°C$ are all polycrystalline GaSe. Results of the analysis of patterns using computer software with the (A.S.T.M.) cards are given in Table I. The Table indicates the polycrystalline nature of a hexagonal structure. The calculated results are in good agreement with the measured values and those reported in literature [16].

The most intensive diffraction peak of the polycrystalline films corresponds to the (0,0,2n) plane and these types of reflections are considerably dominant in the samples suggesting a preferable orientation of crystallites with c-axis parallel to the substrate [16]. The best fit of the (0, 0, l) reflections gives the cell parameters of $a = 3.750$ °A, $c = 15.940$ °A and $c/a = 4.250$ which indicates that these films are β-GaSe with hexagonal lattice and these results are consistent with the values for GaSe given in A.S.T.M. cards and reported in literature [9, 16].

3.2. Electrical conductivity and Hall mobility of GaSe thin films

Both the sign of Hall coefficient and hot probe techniques indicate that GaSe thin films exhibited the p-type conductivity. The room temperature conductivity of the films grown at $T_s = 200°C$ was found to be around $\sim 10^{-9}$ $(\Omega\text{-cm})^{-1}$ which makes electrical characterizations of these films difficult due to instrumental limitations-the used Keithley apparatus (Keithley 614 multi-meter and Keithley 220 current source) are not capable of measuring resistances greater than 10^{12} Ω-. The room temperature conductivity of GaSe thin films grown at $T_s = 300°C$ was found to vary in between 8.4×10^{-5} and 4.8×10^{-4} $(\Omega\text{cm})^{-1}$ for different films prepared under the same conditions. Thus, the data reported here is for a representative sample obtained at $T_s = 300°C$. The above reported values indicate that the conductivity of the films increases with increasing substrate temperature. This increase of the conductivity is attributed to the formation of the polycrystalline films as observed from the X-ray analysis. The room temperature Hall mobility (μ) and carrier concentration (p) of the films evaporated at $T_s = 300°C$ are found in between 12–10 cm^2 V^{-1} s^{-1} and 4.4×10^{13}–3.0×10^{14} cm^{-3}, respectively.

TABLE I Analysis of the X-ray patterns for GaSe thin films grown at $T_s = 300°C$

Measured d (°A)	Calculated d (°A)	A.S.T.M. d (°A)	A.S.T.M. I/I_0	Measured I/I_0	A.S.T.M. hkl	Calculated hkl
7.963	7.960	7.964	62	4	002	002
4.004	3.980	3.990	100	100	004	004
1.877	1.875	1.874	17	10	110	110
1.597	1.591	1.591	21	8	202	202

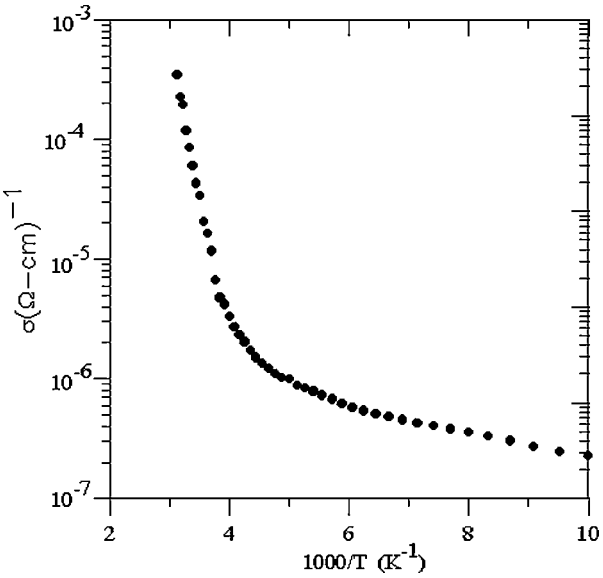

Figure 2 Variation of conductivity with reciprocal temperature for GaSe thin films grown at $T_s = 300^\circ$.

To establish the dominant conduction mechanism, the temperature dependence of conductivity was studied in the temperature range 320–100 K. For the polycrystalline films, the conductivity decreases with decreasing temperature as shown in Fig. 2. The variation of the conductivity with temperature becomes weak below 180 K.

To investigate the transport mechanisms in the deposited films, the conductivity-temperature dependence is analyzed according to the following three possible conduction mechanisms;

i. Thermionic emission over the grain boundary potential model proposed by Seto [22] in which the conductivity is given by,

$$\sigma\sqrt{T} = \sigma_0 \exp\left(-\frac{E_\sigma}{kT}\right) \tag{1}$$

where σ_0 is the pre-exponential factor and E_σ is the conductivity activation energy.

ii. Thermally assisted tunnelling [23] for which σ varies as T^2 according to expression,

$$\sigma = \sigma_1\left(1 + \frac{F^2}{6}T^2\right) \tag{2}$$

where σ_1 and F are constants.

iii. Mott's variable range hopping [24], the expression for the conductivity at low temperatures is given by,

$$\sigma\sqrt{T} = \sigma_2 \exp\left(-\left(\frac{T_0}{T}\right)^{1/4}\right) \tag{3}$$

where, $$\sigma_2 = e^2 a^2 \nu_{\text{ph}} N(E_F) \tag{4}$$

and $$T_0 = \frac{\lambda\gamma^3}{kN(E_F)}. \tag{5}$$

Here a is the hoping distance, ν_{ph} is the phonon frequency ($\sim 10^{12}$, typically) obtained from the Debye temperature and λ is a dimensionless parameter ($\sim$18.1). Two other parameters R, W the hopping distance and the average hoping energy respectively, are given elsewhere [25, 26].

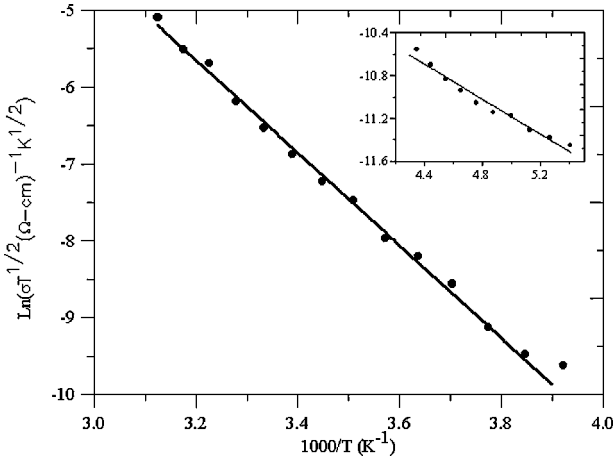

Figure 3 Variation of $\text{Ln}(\sigma T^{1/2}) - T^{-1}$ in the temperature region of 320–180 K.

As illustrated in Fig. 3, in the temperature range 180–320 K the conductivity-temperature variations were found to follow Equation 1 in accordance with the thermionic emission theory. Two different activation energy values, 500/87 meV are obtained above and below 250 K from the slopes of linear $\text{Ln}(\sigma\sqrt{T}) - T^{-1}$ variation, respectively. To check the validity of the tunnelling transport mechanisms $\sigma - T^2$ variations were examined and found to be non-linear indicating that this kind of transport mechanism is not adequate in the studied temperature range. In the low temperature region (below 180 K), the temperature dependence of the conductivity was explained with the Mott's variable range hopping mechanism since the linear $\text{Ln}(\sigma\sqrt{T}) - T^{-1/4}$ plots are obtained as illustrated in Fig. 4. Mott parameters have been calculated using Equations 3–5 and listed in Table II and were found to satisfy Mott's requirements ($\gamma R > 1$ and $W > kT$) for variable range hopping. Thus, below 180 K variable range hopping conduction is likely the transport mechanism. The ratio (T_0/T) which represents the degree of disorder in the samples around a specific temperature is of the order

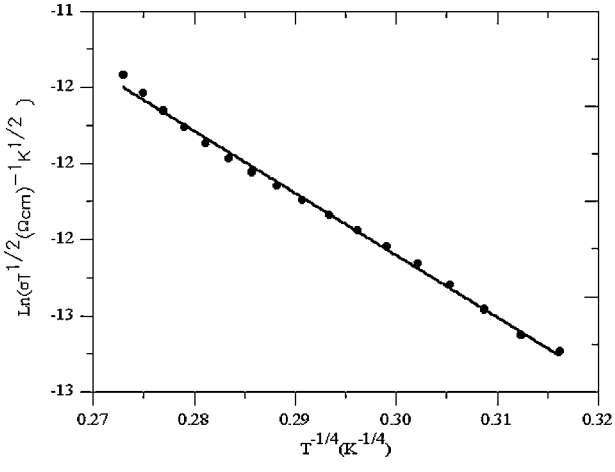

Figure 4 Variation of $\text{Ln}(\sigma\sqrt{T}) - T^{-1/4}$ below 180 K.

TABLE II The calculated electrical and Mott's parameters for GaSe thin films grown at $T_s = 300°C$

σ_{RT} (Ω^{-1} cm^{-1}) $\times 10^{-5}$	8.4
p_{RT} (cm^{-3}) $\times 10^{13}$	4.4
N_t (cm^{-3}) $\times 10^{11}$	1.6
μ_{RT} (cm$^2 V^{-1} \cdot$ s^{-1})	12
E_σ (meV) ($T \geq 250$ K)	500
E_t (meV)	233
$T_0 \times 10^6$ (K)	1.3
$\gamma \times 10^4$ (cm^{-1})	2.2
R(150 K) $\times 10^{-4}$ (cm)	1.6
W(150 K) (meV)	32
γR	3.6
$N(E_F)$ (cm^{-3} eV^{-1})	1.7 $\times 10^{12}$

of 10^3 indicating that the samples are of polycrystalline structure consistent with XRD results.

To our knowledge no work has been carried out to study the transport properties of GaSe thin films for a possible comparison of our results. The room temperature conductivity and mobility values reported here are in good agreement with the values of $\sigma = 2.4 \times 10^{-6}$ $(\Omega\text{-cm})^{-1}$ and $\mu = 10$ cm^2 V^{-1} s^{-1} reported by Gurbulak *et al*. for p-type undoped GaSe single crystals [10]. The values of the activation energy obtained from the conductivity measurements agree well with $E_\sigma = 560$ meV for Na-intercalated GaSe single crystals above 300 K [14].

3.3. Space charge limited current studies in GaSe thin films

The I–V characteristics of the GaSe thin films grown at $T_s = 300°C$ was measured in the temperature region of 240–320 K at high voltages up to 400 V for the SCLC studies. Fig. 5 shows the logarithmic current density-voltage (J-V) plots at different temperatures. At low voltages, the J-V relation is linear, corresponding to ohmic region. For the voltages greater than 100 V, J becomes proportional to V^2 indicating the onset of space charge limited current.

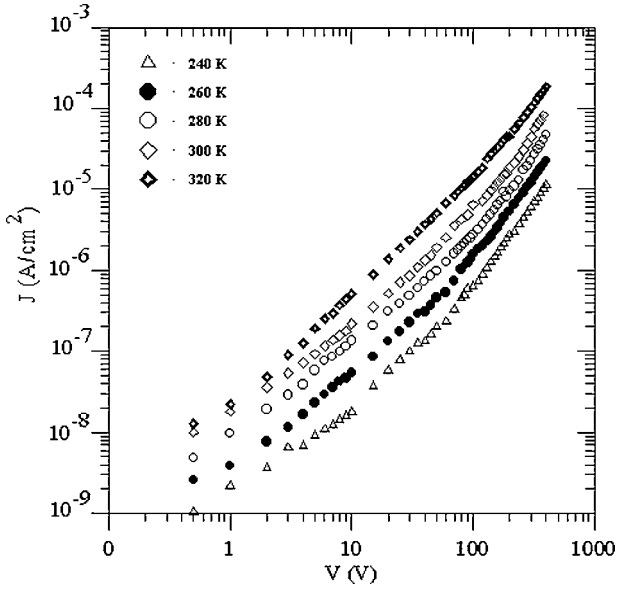

Figure 5 The current density-voltage (J-V) plots at different temperatures.

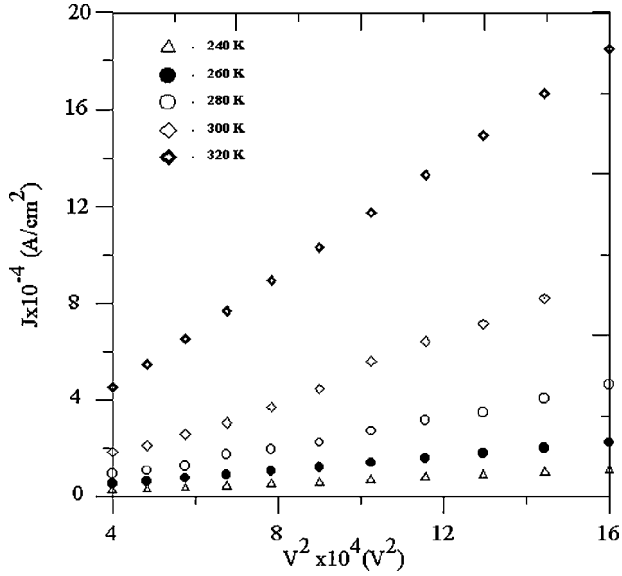

Figure 6 J-V^2 plots at different temperatures in the trap filled region.

The space charge limited current as a function of applied voltage for single carrier injection is given by [27]

$$J = \frac{9}{8}\theta\mu\varepsilon\frac{V^2}{L^3} \tag{6}$$

where μ is the mobility, ε the dielectric constant of the material, L is the distance between the electrodes and θ the ratio of the free to trapped hole density in the material and given by,

$$\theta = \frac{gN_v}{N_t}\exp\left(-\frac{E_t}{kT}\right) \tag{7}$$

In this expression, N_v is the effective density of states for the valance band, N_t the hole trap density, g is the degeneracy factor and E_t is the trap energy.

The J-V^2 plots in the SCLC region at different temperatures are shown in Fig. 6. The figure clearly corresponds to a discrete trapping level, because of the long quadratic region following the ohmic one. From the slopes of linear J-V^2 variations and by substituting the value of the Hall mobility as $\mu = 12$ cm^2 V^{-1} s^{-1}, the distance between the electrodes as 0.15 cm, the dielectric constant value of 10.2, [12]. the θ values were calculated at each temperature. Ln(θ) $- T^{-1}$ plot illustrated in Fig. 7 was found to be linear, the slope of which gives a trap located at a depth 233 meV from the top of the valance band. Assuming the effective density of states in the valance band of GaSe as $N_v = 1.08 \times 10^{19}$ cm^{-3} [12]; using the intercept value obtained from Fig. 7 and Equation 7, the concentration of the trap was obtained as $N_t = 1.6 \times 10^{11}$ cm^{-3}.

Deep trapping levels were observed in GaSe single crystals [14, 29, 30]. Manfredotti *et al*. [13] has reported values of $E_t = 130$–392 meV and $N_t = 1.1$–0.3×10^{13} cm^{-3} for trap depth and concentration respectively. The existence of the discrete deep trap levels was attributed to the association of point-like native defects due to stoichmetric deviations or to extended defect regions like stacking faults or dislocations. The

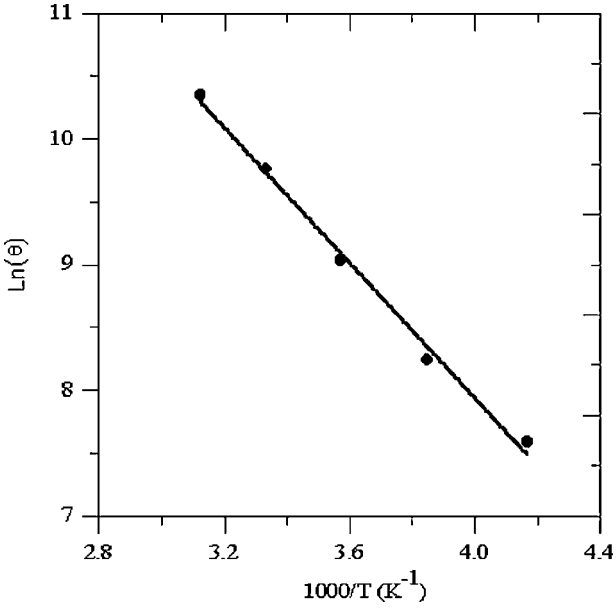

Figure 7 $\mathrm{Ln}(\theta) - T^{-1}$ variation.

values of $E_t = 153$ meV and $N_t = 4.5 \times 10^{10}$ cm^{-3} were also reported for Na-intercalated GaSe single crystal [14], the existence of these levels was attributed to the Na defects in the crystal. The trap level at $E_t = 233$ meV with concentration $N_t = 1.6 \times 10^{11}$ cm^{-3} obtained in this study could be attributed to the point like native defects, due to the stoichiometric deviations during the growth process [13].

The above reported several doping possibilities to produce p-type GaSe thin films and proposed that the Ga vacancies are the most likely to produce p-type conductivities. Thus, the future work is to try to produce GaSe thin films with excess Ga. The purpose of which is to change the nature of the films.

4. Conclusion

In this study, the GaSe thin films were deposited onto glass substrates by the thermal evaporation technique at $T_s = 200$°C and $T_s = 300$°C using GaSe single crystals as a source material. The XRD studies revealed that the films grown at 200°C are amorphous and whose deposited at 300°C have polycrystalline nature with hexagonal lattice structure. To deduce the dominant conduction mechanisms, the temperature dependent conductivity data were analysed by using the thermionic emission theory, variable range hopping and tunnelling. It is concluded that in between 180 K and 320 K the thermionic emission of charged carriers over the grain boundaries and Mott's variable range hopping below 180 K are the dominant transport mechanisms in these films. A hole trap energy with $E_t = 233$ meV and density $N_t = 1.6 \times 10^{11}$ cm^{-3} obtained from space charge limited current measurements.

References

1. P. A. LEE, in "Physics and Chemistry of Materials With Layered Structures: Optical and Electrical Properties," Vol. 4 (Reidel, Boston, 1976) p. 76.
2. A. ARUCHAMY, in "Photoelectrochemistry and Photovoltaics of Layered Semiconductors" (Kluwer Academic Publishers, The Netherlands, 1992).
3. T. TAMBO and C. TATSUYAMA, *Surface Sci.* **222** (1989) 343.
4. G. J. HUGHES, A. MCKINLEY, R. H. WILLIAMS and I. T. MCGOVERN, *J. Phys.* **C17** (1982) L159.
5. A. CASTELLANO, *Appl. Phys. Lett.* **48** (1986) 298.
6. C. MANFREDOTTI, R. MURRI, A. QUIRINI and L. VASANELLI, *Nuclear Instr. and Methods* **131** (1975) 457.
7. A. M. MANCINI, C. MANFREDOTTI, R. MURRI, A. RIZZO, A. QUIRINI and L. VASANELLI, *IEEE Trans. on Nucl. Sci.* **NS-23** (1976) 189.
8. N. B. SINGH, R. NARAYANAN, A. X. ZHAO, V. BALAKRISHNA, R. H. HOPKINS, D. R. SUHRE, N. C. FERNELIUS, F. K. HOPKINS and D. E. ZELMON, *Mater. Sci. Eng.* B **49** (1977) 243.
9. A. KUHN, A. CHEVY and R. CHEVALIER, *Phys. Status Solidi* (a) **31** (1975) 469.
10. B. GURBULAK, M. YILDIRIM, S. TUZEMEN, H. EFEOGLU and Y. K. YOGUTCU, *J. Appl. Phys.* **83** (1998) 2030.
11. V. AUGELLI, C. MANFREDOTTI, R. MURRI and L. VASANELLI, *Phys. Rev.* **B17** (1978) 3221.
12. B. G. TAGIEV, G. M. NIFTIYEV, S. M. BASHIROV and F. SH. AYDAEV, *Solid State Commun.* **50** (1984) 689.
13. C. MANFREDOTTI, A. RIZZO, C. DE BLASI, S. GALASSINI and L. RUGGIERO, *J. Appl. Phys.* **46** (1975) 4531
14. M. A. OSMAN, M. A. ELOSELY and A. A. GADALLA, *Physica* B **252** (1998) 216.
15. I. M. CATALAN, A. CINGOLINI, A. MINAFRA and C. PAORICI, *Opt. Commun.* **24** (1978) 105.
16. M. B. THOMAS, *Thin Solid Films* **8** (1971) 273.
17. M. YUDASAKA and K. NAKANISHI, *ibid.* **156** (1984) 145.
18. K. UENO, M. KAWAYAMA, Z. R. DAI, A. KOMA and F. S. OHUCHI, *J. Crys. Growth* **207** (1999) 69.
19. A. KOÉBEL, Y. ZHENG, I. F. PÉTROFF, M. EDDRIEF, VINH LE THANH and C. SÉBENNE, *ibid.* **154** (1995) 269.
20. M. PARLAK and Ç. ERÇELEBI, *J. Matt. Sci.: Matter. Elec.* **10** (1999) 313.
21. A. F. QASRAWI, I. GUNAL, ÇERÇELEBI, *Crys. Res. Tech.* **35** (2000) 1077.
22. J. Y. SETO, *J. Appl. Phys.* **46** (1975) 5247.
23. M. V GARCIA-CUENCA, J. L. MORENZA and J. ESTEVE, *ibid.* **56** (1984) 1738.
24. N. F. MOTT and E. A. DAVIS, "Electronic Process in Non Crystalline Materials" 2nd ed. (Clarendon Oxford, 1979).
25. D. K. PAUL and S. S. MITTRA, *Phys. Rev. Lett.* **31** (1973) 1000.
26. R. M. HILL, *Phil. Mag.* **24** (1971) 1307.
27. M. A. LAMPERT and P. MARK, "Current Injection in Solids" (Academic Press, New York, 1970).

Received 26 February
and accepted 13 December 2002